ARMY RESEARCH LABORATORY

Nanocomposite Interphases for Improved Transparent Polymer Composite Materials

by Daniel J. O'Brien, Jason Robinette, James R. Heflin, and Jason Ridley

ARL-TR-4527   **August 2008**

NOTICES

Disclaimers

The findings in this report are not to be construed as an official Department of the Army position unless so designated by other authorized documents.

Citation of manufacturer's or trade names does not constitute an official endorsement or approval of the use thereof.

Destroy this report when it is no longer needed. Do not return it to the originator.

Army Research Laboratory
Aberdeen Proving Ground, MD 21005-5069

Nanocomposite Interphases for Improved Transparent Polymer Composite Materials

Daniel J. O'Brien and Jason Robinette
Weapons and Materials Research Directorate, ARL

James R. Heflin and Jason Ridley
Virginia Polytechnic Institue and State University

1. REPORT DATE (DD-MM-YYYY)	2. REPORT TYPE	3. DATES COVERED (From - To)
August 2008	Final	October 2006–September 2007

4. TITLE AND SUBTITLE	5a. CONTRACT NUMBER
Nanocomposite Interphases for Improved Transparent Polymer Composite Materials	
	5b. GRANT NUMBER
	5c. PROGRAM ELEMENT NUMBER

6. AUTHOR(S)	5d. PROJECT NUMBER
Daniel J. O'Brien, Jason Robinette, James R. Heflin,[*] and Jason Ridley[*]	H84
	5e. TASK NUMBER
	5f. WORK UNIT NUMBER

7. PERFORMING ORGANIZATION NAME(S) AND ADDRESS(ES)	8. PERFORMING ORGANIZATION REPORT NUMBER
U.S. Army Research Laboratory ATTN: AMSRD-ARL-WM-MA Aberdeen Proving Ground, MD 21005-5069	ARL-TR-4527

9. SPONSORING/MONITORING AGENCY NAME(S) AND ADDRESS(ES)	10. SPONSOR/MONITOR'S ACRONYM(S)
	11. SPONSOR/MONITOR'S REPORT NUMBER(S)

12. DISTRIBUTION/AVAILABILITY STATEMENT

Approved for public release; distribution is unlimited.

13. SUPPLEMENTARY NOTES

[*]Department of Physics, Virginia Tech, Blacksburg, VA 24060

14. ABSTRACT

The U.S. Army has a critical need for a lighter, more varied array of visibly transparent materials which are currently limited to a handful of polymers and ceramics. This limitation restricts the design of lightweight transparent laminates since only a narrow range of mechanical properties are available, and the proper design of these structures often relies on the engineer's ability to specify the acoustic impedance of each layer. Composite materials offer the ability to tailor mechanical properties but, due to scattering at multiple interfaces, are not typically transparent unless the refractive indices (RI) of composite constituents (e.g., glass fibers and polymer matrix) are well matched. In these cases, sufficient index matching exists over a relatively narrow temperature range since the matrix RI is highly temperature dependent. In this report, we demonstrate improved temperature performance in a model glass fiber-solvent composite by coating conventional micron-sized glass fibers with glass nanoparticles. After infiltration with a model matrix material, the nanoparticles provide an intermediate refractive index interphase that "smoothes" any step change in RI that develops between the matrix and glass fibers.

15. SUBJECT TERMS

composite, transparent materials, refractive index, nanomaterials, nanocomposite, coating, nanoparticle, self assembly, transparent armor

16. SECURITY CLASSIFICATION OF:			17. LIMITATION OF ABSTRACT	18. NUMBER OF PAGES	19a. NAME OF RESPONSIBLE PERSON Daniel J. O'Brien
a. REPORT	b. ABSTRACT	c. THIS PAGE	UL	32	19b. TELEPHONE NUMBER (Include area code)
UNCLASSIFIED	UNCLASSIFIED	UNCLASSIFIED			410-306-0843

Contents

List of Figures

List of Tables

INTENTIONALLY LEFT BLANK.

1. Objective

The objective was to develop a transparent polymer composite material for which optical clarity is insensitive to temperature. Such a material will aid researchers in the development of a new class of transparent armor materials.

2. Introduction

2.1   Background

The U.S. Army has a critical need for a lighter, more varied array of visibly transparent materials which are currently limited to a handful of polymers and ceramics. This limitation restricts the design of lightweight transparent laminates since only a narrow range of mechanical properties are available to laminate engineers. Presently, to satisfy performance requirements, minimize weight, and maintain transparency, these systems consist of a laminated stack of materials with widely varying mechanical properties. Each material is selected to perform specific functions and must also work as part of the system to defeat a given threat. In order for the laminate to work efficiently, stress waves must be transferred from one layer to the next (*1*, *2*), and the proper design of these structures often relies on the engineer's ability to specify the density and stiffness of each layer. For systems that do not require transparency, polymer composites are a natural choice for applications requiring tailored material properties. Unlike monolithic materials, polymer composites offer additional energy-absorbing damage modes such as fiber breakage and fiber pullout that make them attractive for lightweight armor applications. Unfortunately, due to scattering at multiple interfaces, composite materials are not typically transparent.

Composite materials can be made transparent by either reducing the reinforcement size to significantly below the wavelength of light or matching constituent indices of refraction. Reducing the reinforcement size has been tried with some success by several researchers. Newly developed clay- or nanofiber-based polymer nanocomposites are often transparent since the characteristic size of the reinforcement is much less than the wavelength of incident light. However the volume fraction of reinforcement in these systems is very low and does not provide a significant increase in stiffness and density over neat polymers. It is also possible to make a transparent composite by filling a nanoporous glass with monomer and polymerizing *in situ*, an approach that was successfully implemented in a previous Director's Research Initiative (DRI) study (*3*). With this, method, however, the reinforcement volume fraction and morphology is limited by the process used to manufacture the porous structure.

The alternative rout to transparency, refractive index matching, is difficult since the indices must be matched to approximately the third decimal place (*4*), and transparency becomes increasingly sensitive to index variations as volume fraction increases. For example, Iba and Kagawa (*5*) showed that for $v_f = 0.10$, the transmittance decreases by 20% for a fiber-matrix index mismatch of only 0.0005. The problem is further complicated by the stress- and temperature-dependence of the refractive index. Due to processing-induced residual stresses, a given glass and polymer system may individually have identical indices but become index mismatched after fabrication into a composite. Furthermore, in glass-reinforced systems the index of the polymer matrix changes much faster with temperature than that of the fibers, and in rubber-toughened polymers the index of the rubber phase changes much faster than that of the matrix. Therefore, as figure 1 shows, these index-matched systems are transparent only over a narrow temperature range (*6*).
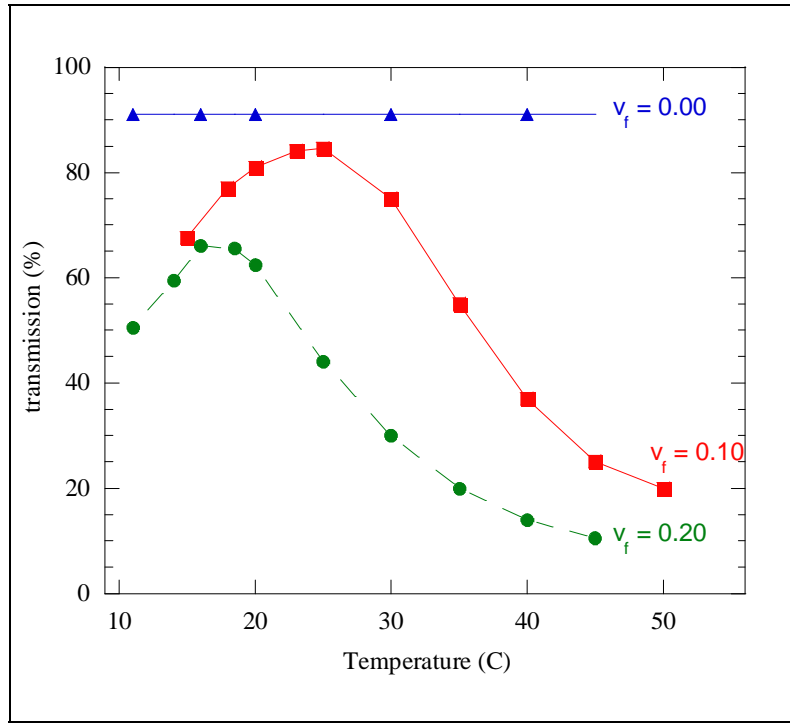
Figure 1. Temperature-dependent transmission of optical glass/poly(methyl methacrylate) composite for various fiber volume fractions (*6*).

In this work we attempt to mitigate this temperature-dependent transparency problem through a combined nanocomposite/refractive index matching approach. Obvious applications for lightweight transparent materials include face shields and windows (both visible and IR transmission). Transparent polymer composites could be used as replacements for polycarbonate face shields. Applied to the ceramic-based systems designed to defeat more significant threats, transparent polymer composites could provide superior backing sheets or interface layers.

2.2 Our Approach

In this work, we will improve the temperature-dependent performance of index-matched transparent glass-polymer composite materials by incorporating a nanocomposite interphase between the bulk polymer and glass reinforcement constituents. As shown in figure 2, in conventional composite materials the refractive indices are matched at one temperature only, T_{match}. However, as the temperature changes, the refractive index mismatch increases and diminishes the optical performance of the composite. In this work, a nanocomposite interphase will be designed and incorporated so that its refractive index will always be between that of the matrix and glass, regardless of temperature.
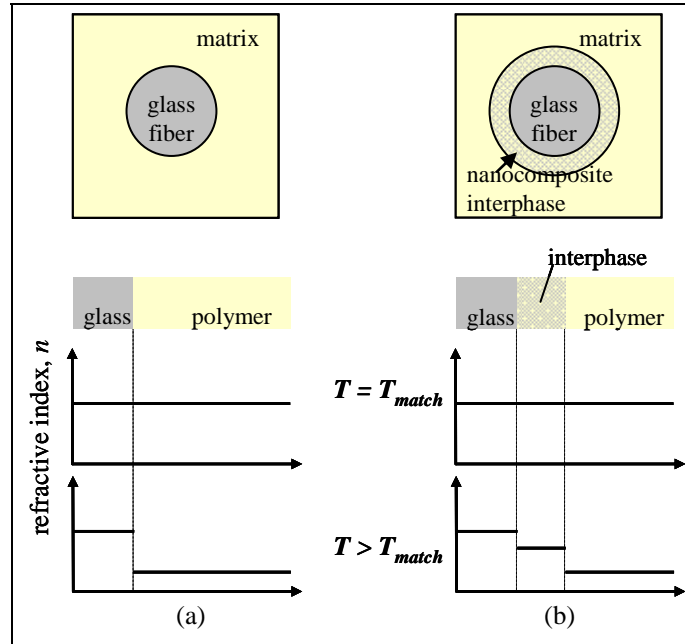
Figure 2. Schematic of glass-polymer composite without (a)
and with (b) incorporated nanocomposite interphase.

Caseri showed that particle size should be reduced to below ~50 nm in a nanocomposite in order maintain transparency with relaxed restrictions on refractive index matching (7). In this size regime, with characteristics lengths much smaller than the incident wavelengths, light passing through the interphase will be less susceptible to scattering, and the region will behave as an optically homogeneous material with a refractive index (n_i) that is essentially the volume-averaged refractive index of its constituents (8). Therefore, if the nanocomposite interphase is composed of the same glass and polymer as the conventional composite with refractive indices n_g and n_p, respectively, then

$$n_i(T) = v_g n_g + (1 - v_g) n_p(T), \tag{1}$$

3

where v_g is the glass volume fraction in the nanocomposite interphase. Assuming that the change in the refractive index of glass with temperature is negligible, the temperature dependence of the interphase refractive index is dominated by the matrix. Therefore, any change in the refractive index of the matrix due to temperature variation will result in a change in the refractive index of the interphase to a value between that of the reinforcement and the bulk matrix. This will serve to smooth the transition between the refractive index of the matrix and bulk, reducing the light scattered by the reinforcing fibers.

Two approaches were used for incorporating the nanocomposite interphase into the composite. In the first, 20 nm were deposited onto the surface of the conventional micron-sized glass fibers by dipcoating in a colloidal silica sol. The coating thickness is controlled through the dip time. Later, during composite processing, the particles are infiltrated with the matrix resin to complete the nanocomposite interphase. In the second approach, alternating layers of silica nanoparticles and polymer will be deposited onto the glass surface through ionic self assembly (*9*). In this technique, the substrate to be coated is alternately dipped in positively and negatively charged solutions of polymer or ceramic nanoclusters that are electrostatically attracted to the surface. Many layers will be deposited in order to reach the desired thickness of the nanocomposite interphase. As with the first approach, the process results in a porous coating that is infiltrated during composite processing. A major advantage of the second approach is the ability to vary the composition of the deposited layers through the thickness to produce a structure with a graded refractive index in contrast to the step change in index depicted in figure 2.

Ionic self assembly for manufacturing nanocomposites on substrates have already been demonstrated. Heflin and coworkers have demonstrated highly effective antireflection coatings using ionic self-assembly of silica nanoparticles (*9*). In this case, a low refractive index of 1.30 is achieved since the void space between the nanoparticles is not filled with a polymer matrix. In the proposed work, a refractive index between that of the glass and polymer will be obtained by infiltration with the matrix resin. Self-assembled monolayer-based nanocomposites have also received attention for applications such as a technique for engineering the refractive index of coatings (*10*). Furthermore the technique has been used on optical fibers to produce Bragg grating's from alternating high- and low-refractive index layers (*11*). Sandrock and coworkers developed a tunable refractive index nanolayered material using a co-extrusion process (*8*). Shiue et al. coated optical fibers with a silica nanoparticle-polymer composite to improve the mechanical properties of the fibers (*12*). However, to our knowledge, the techniques have not been used in structural composites for the purpose of matching refractive indices of fibers and matrix for transparent composite applications.

In the sections that follow, a model that predicts the temperature-dependent behavior of nanoparticle-coated glass-polymer composites will be presented first and compared to conventional composite materials. Next, two different particle deposition techniques will be presented, ISAM and the aggregation of colloidal silica, and used to improve the transparency of planar- and fiber-based model composites.

3. Modeling

In order to prove the concept, the nanocomposite interphase was first applied in a planar geometry where the fraction of incident light energy, R, reflected at a boundary between materials of refractive indices n_1 and n_2 is given by:

$$R = \left(\frac{n_1 - n_2}{n_1 + n_2} \right)^2 . \tag{2}$$

In this experiment, the interphase at various thicknesses was applied to a conventional glass slide and then infiltrated with liquids of various refractive indices. A spectrophotometer was used measure the reflected intensity from specimens with and without the nanocomposite interphase.

A scattering model was used to predict the nanocomposite coating's ability improve transparency in a conventional, index matched composite. The solution for transmitted intensity through a collection of spheres suspended in a matrix is well known (*13*). The attenuation through any material can be described by Beer's law,

$$I_T = I_0 e^{At} , \tag{3}$$

where I_0 is the intensity of the incident light, A is the attenuation coefficient, and t is the part thickness. The intensity attenuation coefficient is a function of the number of particles as well as particle geometry and constituent optical properties through

$$A = \frac{3 v_f Q}{4r} , \tag{4}$$

where v_f is the volume fraction of particles, r is the particle radius and Q is the scattering efficiency. The scattering efficiency has been calculated for a range of particle types including a coated sphere. The solution for the coated sphere calculates Q as a function r_s, r_c, n_s, n_c, n_m the radius of the sphere, coating, and refractive indices of the sphere, coating, and matrix, respectively. Several implementations of this calculation are freely available as computer codes. In this work, we use a version written in Mathematica (Champaign, IL) (*14*). The transmission through a 1-mm composite slab is calculated for a range of particle volume fractions, coating thicknesses, and matrix refractive index. The local glass volume fraction of the coating in all cases is taken to be 0.50 which gives the coating refractive index as

$$n_c = \frac{(n_g + n_p)}{2} . \tag{5}$$

The particle refractive index is assumed, $n = 1.50$, and the particle diameter is 10 μm a typical values for glass. The matrix refractive index ranges from 1.500 to 1.505. While such a change

in n may seem small, it is large enough to greatly decrease the transparency. The range is also typical of the variation expected over a 50 °C change.

Figure 3 shows the results of the scattering model for a particle volume fraction of 0.10. As expected, the transmission of the through the composite increases as the coating thickness increases. The results indicate that a 1-µm-thick coating is enough to realize a measurable increase in the composite's transparency.
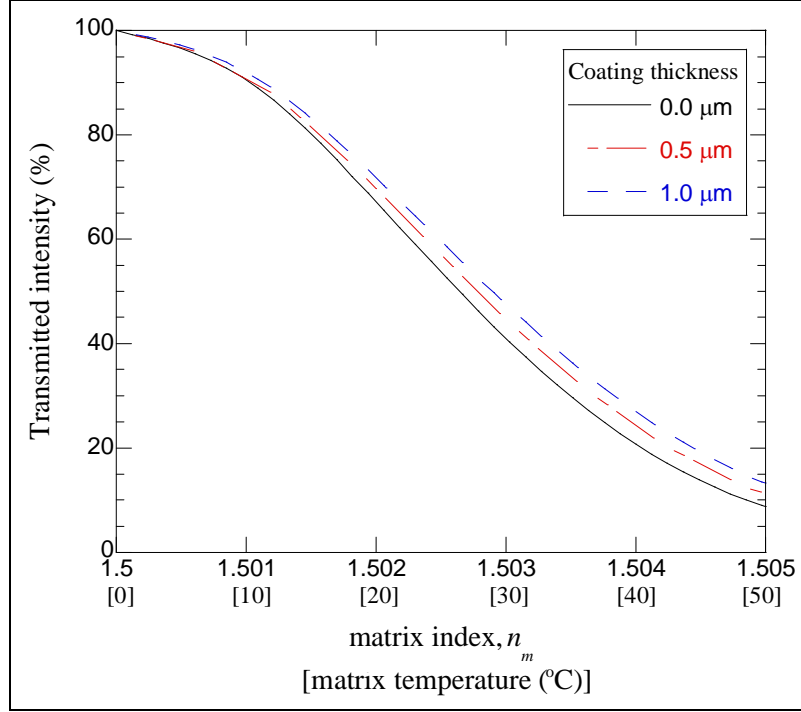
Figure 3. Model prediction for transmission through a 1-mm-thick particle-glass composite for various coating thicknesses as a function of matrix refractive index. The numbers in braces correspond to the temperature change necessary to induce the corresponding change in refractive index. The coating refractive index has an intermediate value between the matrix and the paritcle ($v_f = 0.10$, $n_{particle} = 1.50$).

4. Experiments

Model matrix-glass systems were chosen in order to test the concept of increasing composite transparency with a nanocomposite interphase. A glass-liquid system was chosen to avoid processing difficulties and demonstrate this proof-of-concept. Two types of experiments were conducted. In type 1, coatings were deposited onto glass slides which were then dipped in fluids

of various refractive indices to determine if the coated slides were more or less transparent. A similar experiment, type 2, was conducted with coated fibers except only a single fluid was used and the fluid refractive index was varied by slowly ramping the temperature.

4.1   Ionically Self-Assembled Multilayers, Type 1

Ionically self-assembled multilayers (ISAM) deposition is a relatively simple and effective method for depositing coatings onto a substrate. This method involves the electrostatic attraction of oppositely charged particles to permit film growth. A key advantage based on this principle is that substrates need not have simple geometric constraints; films may be deposited onto curved and large/small surfaces with uniform coverage. It is a wet chemical process, and aqueous polyelectrolyte solutions must be prepared in order to facilitate deposition (polyelectrolyte solution conditions are listed at the end of this document). The substrate is immersed alternately into the polycation and polyanion solutions, with a water rinsing step included after immersion to remove weakly interacting particles. The cycle that constitutes the adsorption of both polycation and polyanion is commonly referred to as a bilayer. To reach certain film thickness criteria, this cycle may be repeated as many times as is necessary. In most ISAM films, it is found that the thickness per number of deposited bilayers remains constant, implying uniform growth.

ISAM methods have been implemented to coat glass slides with coatings of two different thicknesses. The polycation used is poly(allylamine hydrochloride) (PAH). Silica nanoparticles (40-nm particle diameter) in colloidal suspension are used for the polyanion solution. The glass was first RCA-cleaned (treated in base and acid baths) to alter the surface chemistry, putting negative charge on the glass surface. Once this has been done, it is possible to coat the slides via self-assembly. The slides dipped into the PAH solution for 3 min and gently rinsed in two or three beakers containing deionized water. After this the glass substrate immersed into the silica nanoparticle solution for 3 min, and rinsed similarly. This completes a single bilayer. A total of 5 and 10 bilayers were fabricated to create a films with thicknesses of around 100 and 200 nm, respectively. Finally, the slides were dried with N_2 to remove water. A similar method was used to coat 9-μm fused silica fibers with 25 bilayers at a thickness of ~500 nm.

The polyelectrolyte solution were prepared from PAH from Sigma-Aldrich: 10 mM PAH ($M_w = 70,000$) is adjusted to a pH value of 7.0 (solution is stirred overnight). Snowtex silica nanoparticles ST-20L from Nissan Chemical received as 20–21 weight-percent glass was diluted by the ratio of 4 parts water to 1 part silica nanoparticles. The initial molarity is 3.76 mol/L; therefore the final molarity of the SiO_2 solution is 0.94 mol/L. The pH of the solution is adjusted to 9.0.

4.2   Colloidal Silica Aggregation, Type 2

Since many of the available glass nanoparticles are fused silica, we chose fused quartz for the fibers in our model system. A common method for coating silicon substrates such as quartz is by

dip-coating them in a colloidal silica sol. In these systems, the microstructure of the silica coatings is strongly dependent on the stability of the sol (*15*). The stability of the colloidal silica was influenced by reducing the pH of the sol. The density of silanol groups on the surface of silica increases as pH decreases. This results in a short range structural interaction dominated by the presence of undissociated silanol groups. Hydrogen bonding between silanols and surrounding water molecules results in the formation of silica aggregates throughout the solution. When introducing the fibers (which contain surface silanol or hydroxyl groups) to the colloidal silica sol, the silica aggregates form hydrogen bonds with the silica surface, thus resulting in a silica-coated fiber. The fibers were subjected to various treatment times at a constant pH to allow for the formation of different aggregate sizes in the solution and different lengths of time for the reaction of silica and the aggregates with the fiber surface. At long enough times, the aggregation size reaches equilibrium in solution and there is no longer a driving force for further bonding of silica.

In this work, a colloidal silica sol was created by adding 10 weight-percent, 20-nm silica (Ludox TMA, Grace Davison, USA) to a 90:10 (v:v) ethanol-water solution where the pH was adjusted to 4.5 with the addition of acetic acid. Immediately after the sol was formed, the fibers were dipped in the solution for times of 1 min, 10 min, 1 hr, 6.5 hr, and 1 day. The fibers were dried for several hours at 100 °C.

4.3   Transmission Measurements

The transmission through the glass slides were measured by using a UV-Vis spectrophotometer (Lambda 25, Perkin Elmer, Waltham, MA). A series of five slides were placed in a fused silica cuvette (93-G-50, Starna Cell Inc, Atascadero, CA) filled with one of several fluids as shown in table 1.

Table 1. Immersion fluids used in testing glass slide transparency.

Fluid	Refractive Index $n_{589nm}^{20^\circ C}$
Air (unfilled)	1.000
Water	1.333
Glycerol-water (50:50)	1.403
Glycerol	1.473

The transmission through the model matrix-glass fiber composites was also measured using a UV-Vis spectrophotometer (Lambda 950, Perkin Elmer) with the fibers immersed in dimethyl sulfoxide (DMSO). DMSO is a liquid that readily infiltrates the porous coatings and has a refractive index that is fairly close to that of fused silica. Most importantly, it has a high thermo-optic coefficient, dn/dt, which results in a large change in transparency over a relatively narrow temperature range. In this experiment, the fibers were coated via colloidal aggregation (type 2, as previously described) and soaked over night in DMSO for 16 to 18 hr. Then, as shown in figure 4, eight fiber tows were assembled length-wise inside the cavity created by a rubber gasket
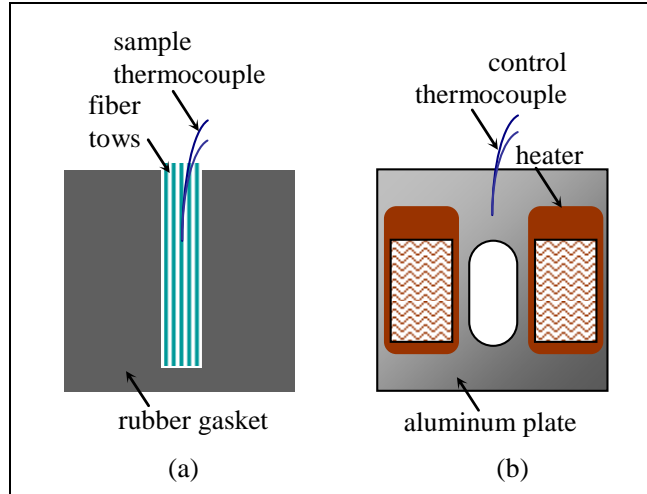
Figure 4. Specimen configuration for model composite
transmission measurements. (a) rubber gasket
containing vertical fiber tows and (b) aluminum
front/back plates. The sample is constructed by
sandwiching the gasket (a) between two 50- ×
75-mm glass slides (not shown) which is, in turn,
sandwiched between the aluminum plates (b).

sandwiched between two glass slides. The fiber, glass slide assembly was sandwiched between
two aluminum plates (70 × 70 × 1.5 mm) which have a 12.5-mm slot to allow for transmission of
the spectrophotometer beam. Two 20-W, 2- × 1-in silicone rubber heaters (model 35765K164,
McMaster-Carr, Robbinsville, NJ) were attached on the outer side of both aluminum plates as
shown, and the temperature was controlled via a thermocouple and temperature controller
(Digitrol II, Glas-Col, Terre Haute, IN). After assembly, the specimen was clamped to the
sample fixture (figure 5) placed inside the spectrometer normal to the beam. The temperature
was then ramped at 0.5 °C/min from room temperature to 100 °C and the transmission was
measured at 589 nm. Additionally, a thermocouple was placed inside the sample just above the
top of the slot in the aluminum. The temperature from this thermocouple was recorded using a
thermocouple reader (Model 54II, Fluke Corp, Everett, WA) and is reported as the sample
temperature in the following results.

5.   Results and Discussion

Figure 6 shows a scanning electron microscope (SEM) image of nanoparticles deposited on a
planar surface via ISAM. As the image shows, the particles ~40 nm in diameter are deposited in
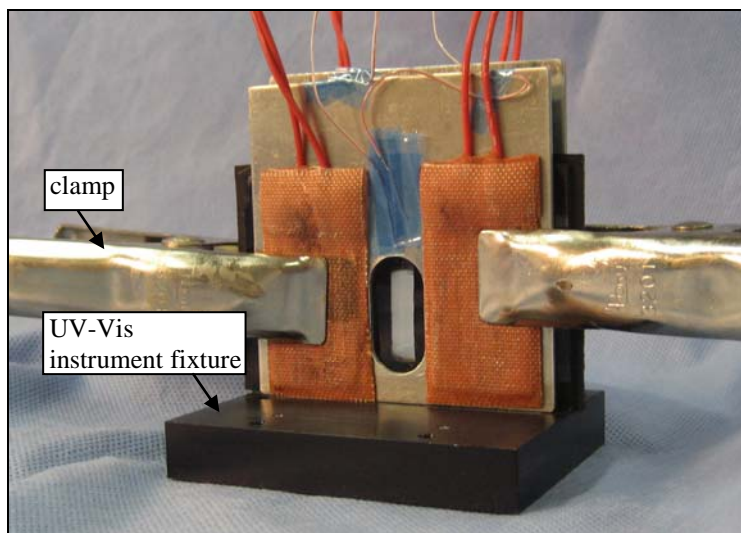a random fashion.

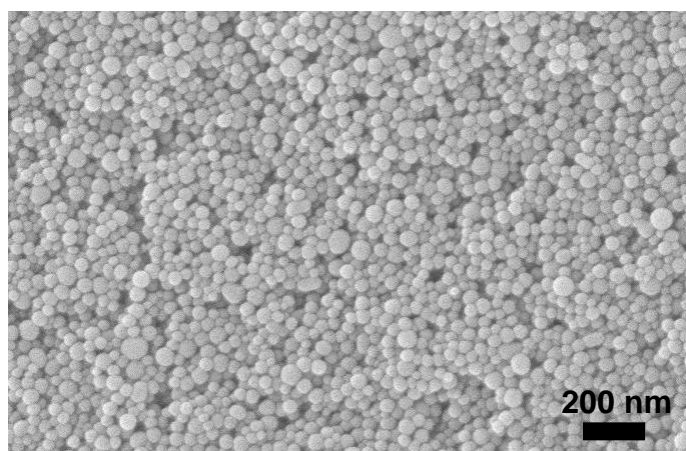Figure 5. Assembled transmission measurement specimen.

Figure 6. SEM image of nanoparticles deposited onto a glass
slide via ionic self assembly.

Figures 7–9 show SEM images of the fibers coated via colloidal silica aggregation soaked for
1 min. Figures 7 and 8 show images of fibers taken from the exterior and interior of the fiber
tows, respectively. Not surprisingly, the particles are more readily deposited onto the exterior
fibers. However, a large number of particles do penetrate the tow. Figure 9, an image of a
fractured fiber end, shows that for this fiber the coating thickness is 100–200 nm. Figure 10
shows the mass uptake of fibers soaked for various amounts of time as well as the estimated
coating thickness. This estimated coating thickness was calculated by assuming that all fibers
were uniformly coated with randomly close packed spheres with a packing factor of 0.6 (*16*).
The calculated thickness agrees well with the thickness observed in figure 9.
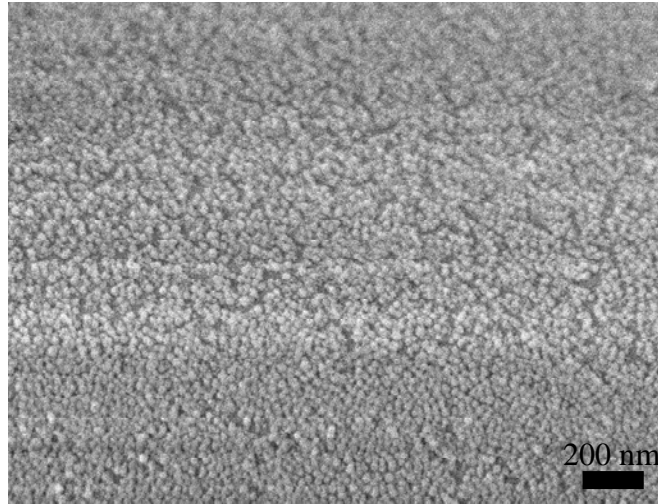
Figure 7. SEM image of fibers coated by colloidal silica
aggregation. The fiber was taken from the outer
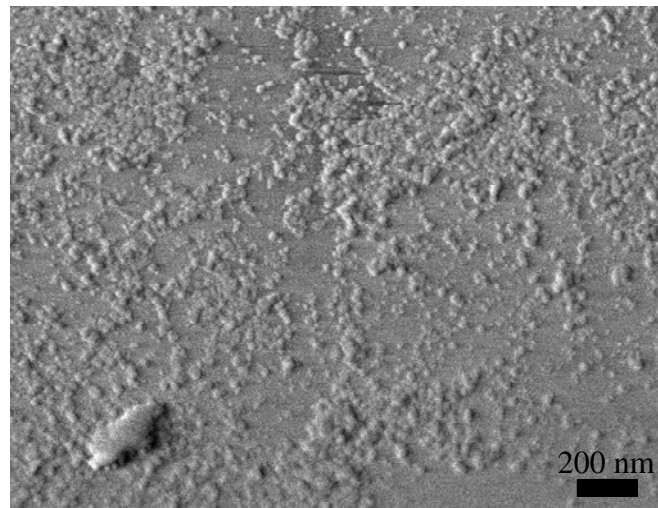edge of the fiber tow.

Figure 8. SEM image of fibers coated by colloidal silica
aggregation. The fiber was taken from the interior
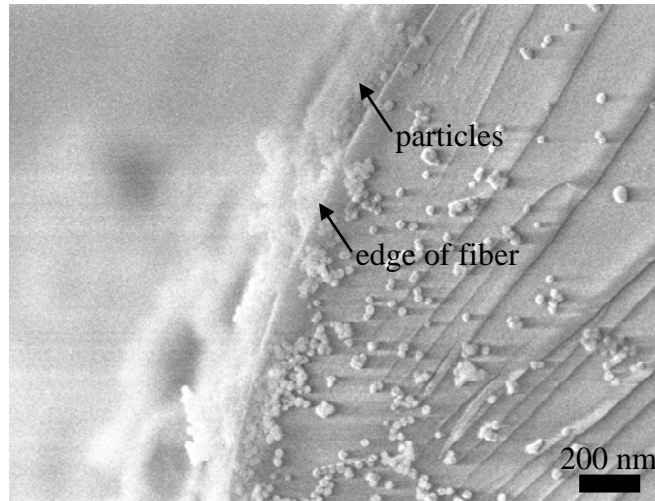of the fiber tow.

Figure 9. SEM image taken along the axis of a fractured coated fiber (coated via colloidal silica aggregation, 1-min soak). Fiber was taken from the exterior of the tow.
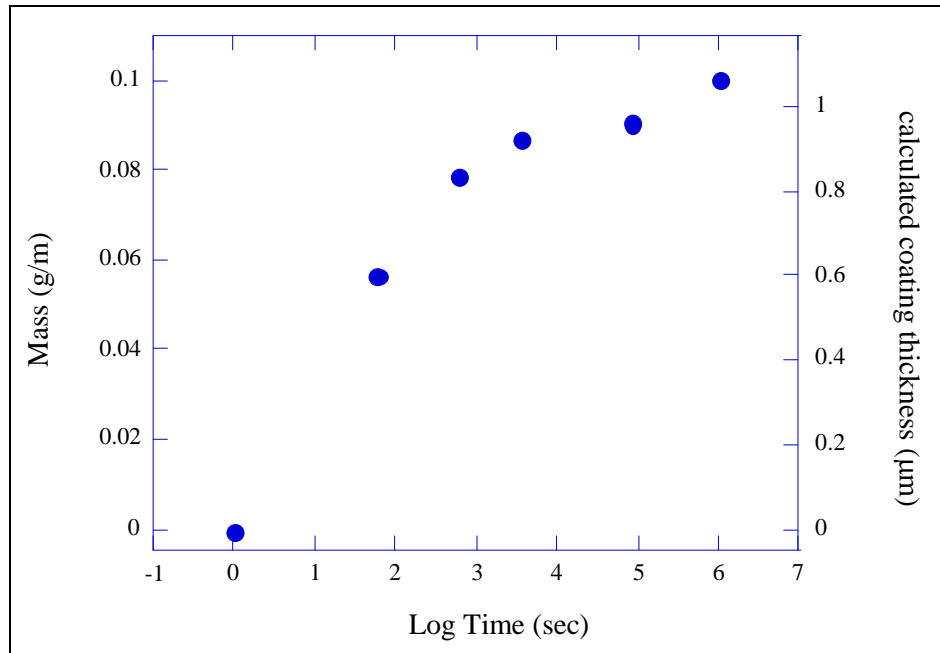

Figure 10. Mass uptake of fiber bundles using colloidal silica aggregation. The coating thickness is calculated by assuming equal coverage on all fibers.

Figures 11–14 show spectrophotometer scans of ISAM coated glass slides immersed in the various refractive index liquids. The thickness of the coating is ~100 and 200 nm for the 5 and 10 bilayers, respectively. The results demonstrate that for this planar geometry the transmission through the composite can be improved through the application of a porous coating that, along with the matrix, forms a nanoporous composite interface that serves to "smear" the optical interface between matrix and glass fiber. For the 5 bilayer specimens, the transmission of the coated slides is relatively flat and always above that of the uncoated slides. For the 10 bilayer case, the transmission shows several interference fringes, a result of the coating thickness equaling some multiple of the spectrophotometer's wavelengths. However, when the coating thickness is outside of this regime, the transmission is relatively flat and an overall increase in transmission is observed. Figure 15 shows the data as a plot of the transmission at a wavelength of 589 nm as a function of the refractive index mismatch. This plot is similar to the expected behavior as the material undergoes temperature changed, resulting in refractive index mismatch. Compared to the uncoated slides, the coated specimens show less dependence on transmission with increasing refractive index mismatch.

Figure 11. Spectrophotometer scans of ISAM coated slides "immersed" in air.
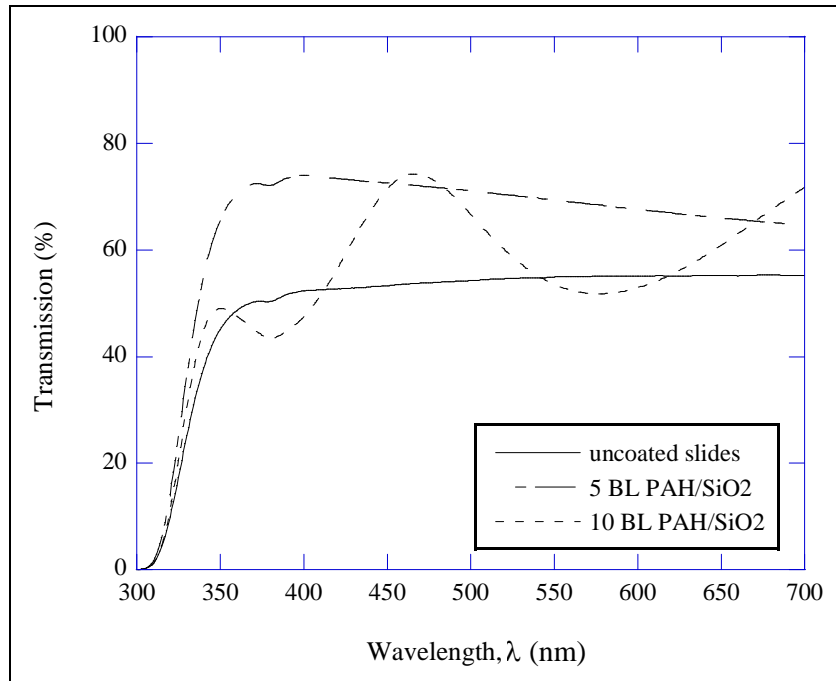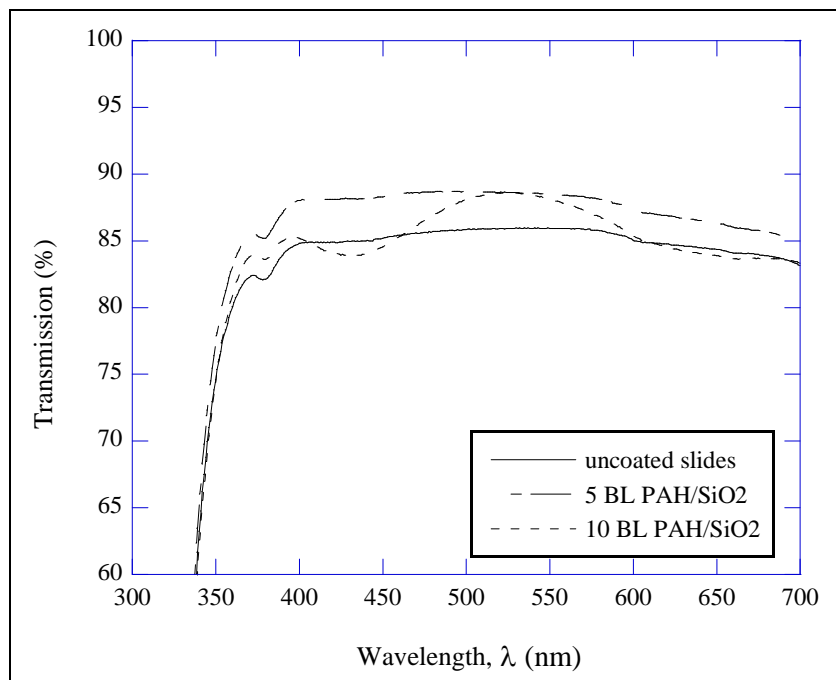
Figure 12. Spectrophotometer scans of ISAM coated slides immersed in water.
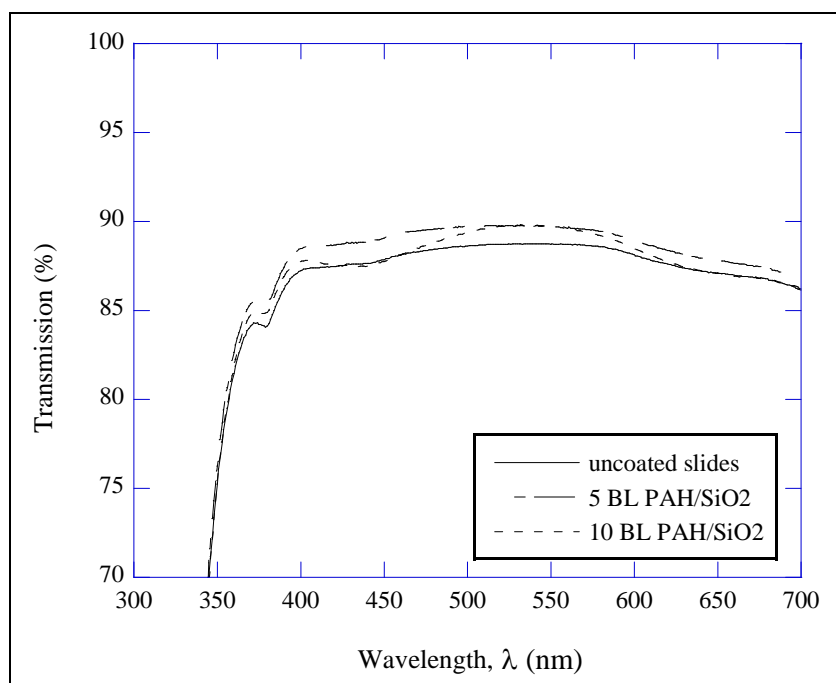

Figure 13. Spectrophotometer scan of ISAM coated slides immersed in
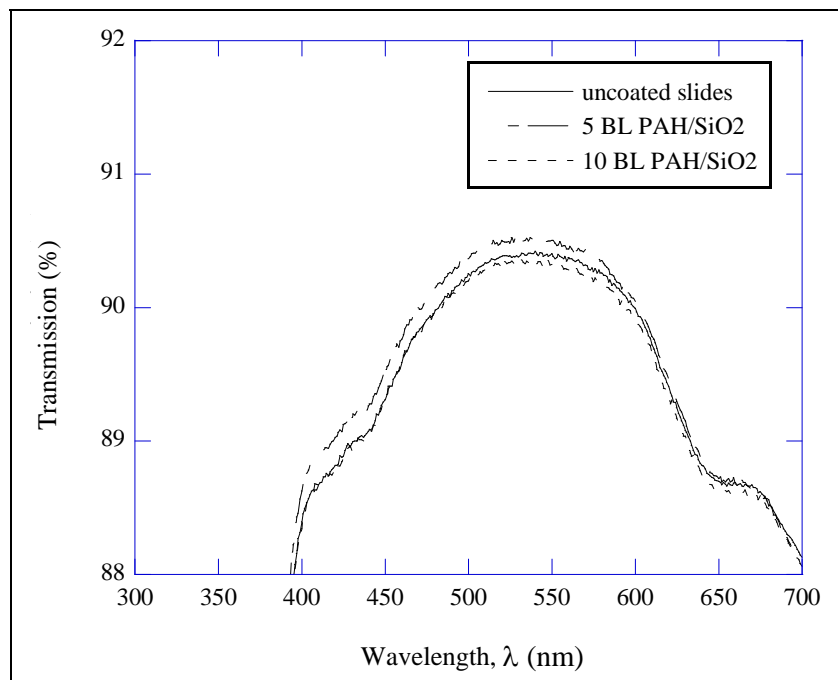water-glycerol (50:50).

Figure 14. Spectrophotometer scans of ISAM coated slides immersed in glycerol.
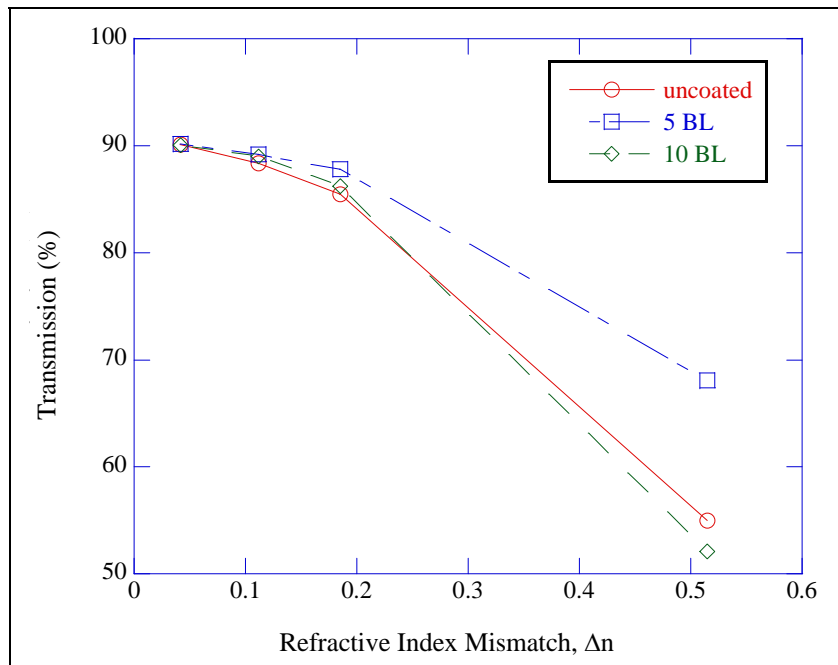

Figure 15.   Transmission at $\lambda = 589$ nm of ISAM coated slides immersed in fluids of a range of refractive indices.

Figure 16 shows that the temperature-dependent transmission through nanoparticle coated, glass fiber/dimethyl sulfoxide (DMSO) composites for fibers soaked in colloidal silica for various amounts of time. Unfortunately, there is considerable scatter among the data in the location of the peak and it is difficult to discern a difference in the temperature-dependent transmission among the various samples. This scatter could be due to variations in the heating rate, as well as the properties of each particular specimen. Lin et al. (*17*) modeled the transmission through conventional glass-polymer composites and found that it is very sensitive to fiber volume fraction, variations in the fibers' refractive index and diameter, as well as the proportion of fibers that are not fully wetted by the matrix. A combination of these factors likely accounts for the scatter in the temperature of maximum transmission as well as the magnitude of the peak. Nevertheless, assuming that thermo-optic coefficient of DMSO is $-5.4 \times 10^{-4}/°C$ (*18*), neglecting the thermo-optic behavior of the glass fibers ($3.5 \times 10^{-6}/°C$), and assuming that the refractive indices of DMSO and fused quartz at 25 °C are 1.476 (*19*) and 1.459 (*20*), respectively, the maximum transmission should occur at 59 °C, in good agreement of that measured here, 64 °C.
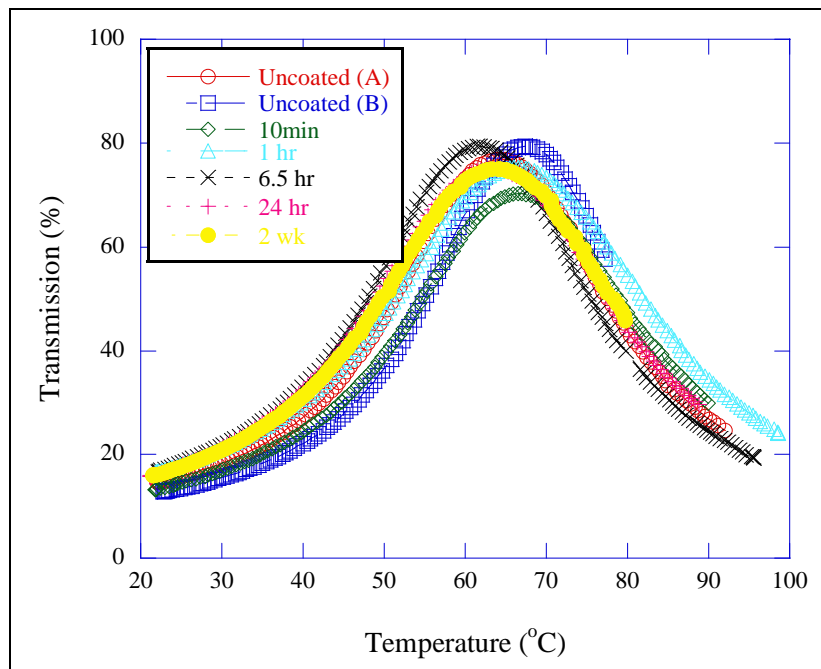
Figure 16. Temperature-dependent transmission through glass fiber/DMSO composites with various coating times.

In order to investigate the coating's effect on the temperature-dependent transmission and eliminate the random variations from sample to sample, the data were replotted on a graph centered about and normalized by the peak transmission. This plot, shown in figure 17, reveals that the Gaussian transmission curve broadens as the coating time (and presumably coating thickness) increases, indicating that the temperature dependent transmission of refractive index matched composites can be improved with nanocomposite interphases. Figure 18 reinforces this

Figure 17. Transmission data after centering the graph about the peak
and normalizing by the peak in transmission.

Figure 18. Transmission data similar to figure 17 with additional data.

17

idea with additional data, and figure 19 shows the transmission at a temperature 20 °C below the peak over the range of deposition times.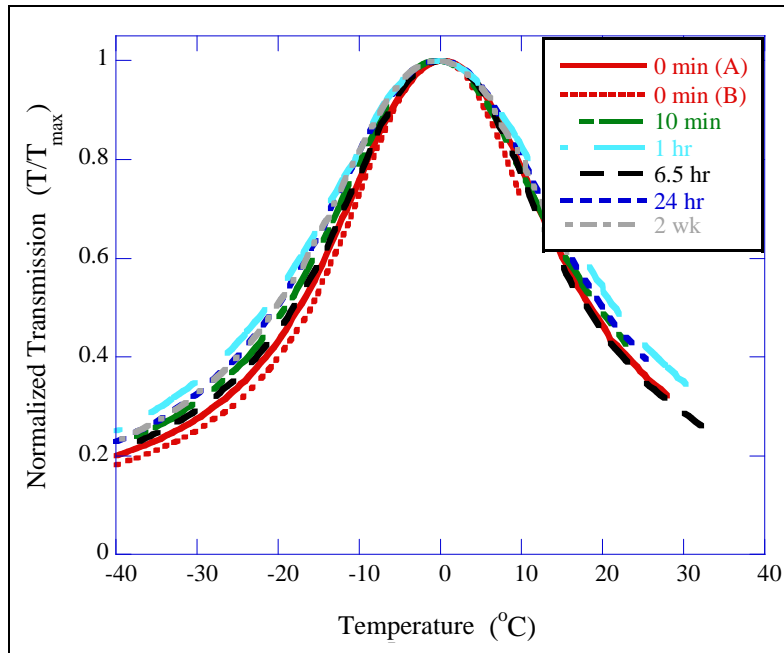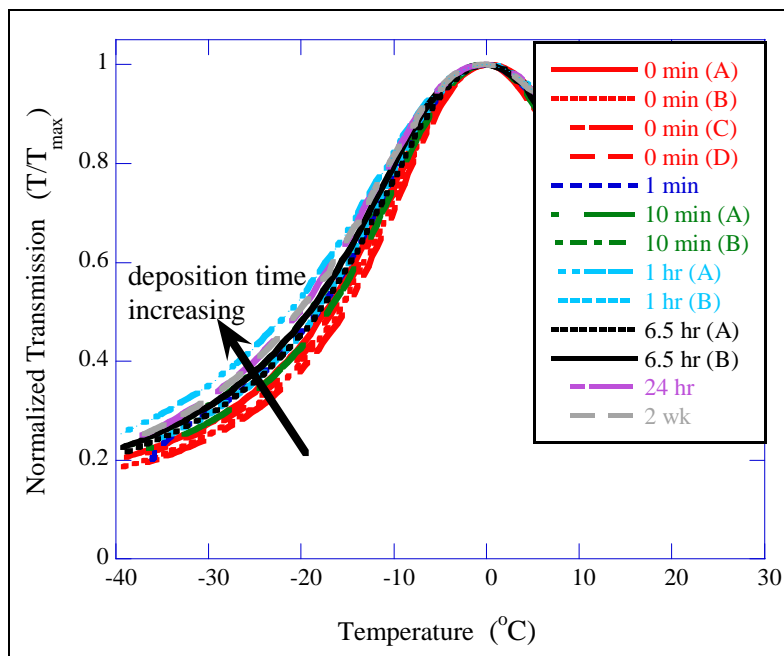 The transmission increases, as expected, from ~40% for uncoated fibers to ~50% for the fibers coated the longest times. The scatter in the transmission with increasing coating time is likely due to a variation in coating thickness as demonstrated by the uncertainty in the mass uptake also shown in figure 19.
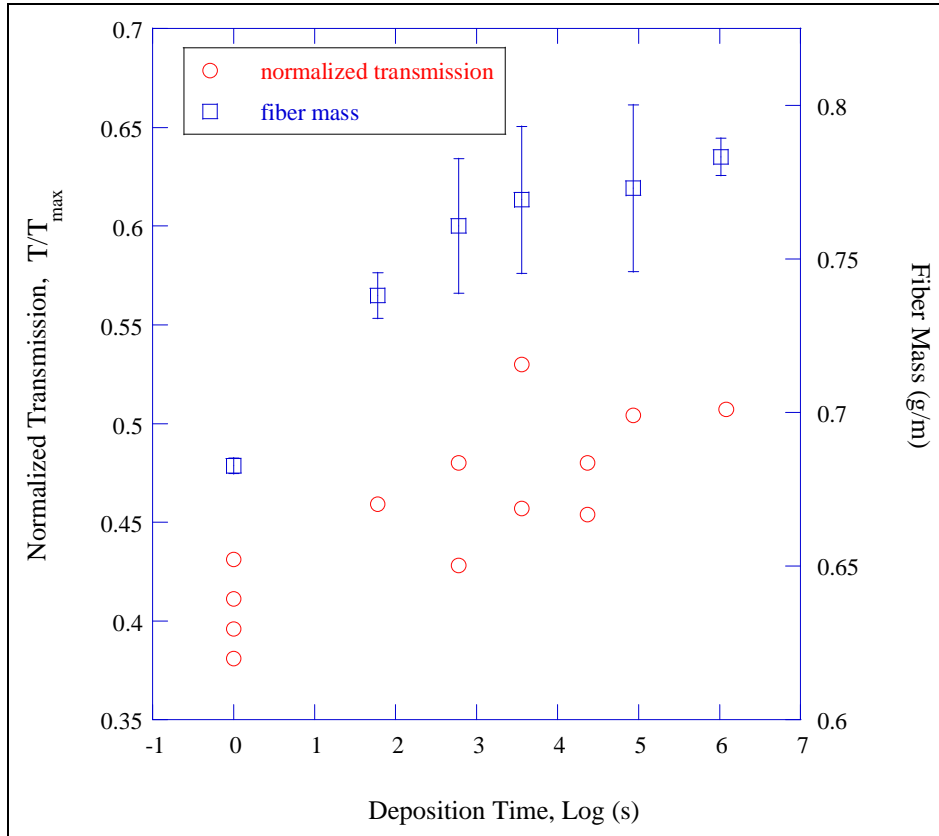
Figure 19. Transmission data from figure 19 plotted for a single temperature 20 °C below the peak in transmission. Also plotted is the fiber mass for the range of deposition times.

6. Conclusions/Future Plans

In this work, we have demonstrated that it is possible to improve the optical performance of refractive-index matched composites by incorporating a polymer-nanoparticle interphase between the matrix (polymer) and reinforcement (glass) phases. In conventional composites, the temperature dependence of the matrix refractive index results in significant mismatch of constituent refractive indices as the temperature is changed. However, since the refractive index

18

of the nanocomposite interphase will assume a value between that of the bulk matrix and the reinforcement without scattering light, it serves to smear the optical boundary between the phases, improving transparency.

Future work will include testing this technique on reinforcements of other geometries such as ribbons and flakes as well as investigating the interphase's effect on composite mechanical properties. The technique must also be extended from the model system studied in this research to polymer-based system such as glass-poly(methyl methacrylate). It is also necessary to investigate different techniques for nanoparticle deposition, including perhaps, deposition during fiber manufacture or before tow construction to improve the coating uniformity throughout the tow.

7.   References

1. Li, Y.; Ramesh, K. T.; Chin, E. S. C. Dynamic Characterization of Layered and Graded Structures Under Impulsive Loading. *International Journal of Solids and Structures* **2001**, *38* (34–35), 6045–6061.

2. Tasdemirci, A.; Hall, I. W. Experimental and Modeling Studies of Stress Wave Propagation in Multilayer Composite Materials: Low Modulus Interlayer Effects. *Journal of Composite Materials* **2005**, *39* (11), 981–1005.

3. O'Brien, D. J.; Juliano, T. F.; Patel, P. J.; McKnight, S. H. *Optically Transparent Nanoporous Glass-polymer Composites*. Army Science Conference, Orlando, FL, 2006.

4. Sato, H.; Iba, H.; Naganuma, T.; Kagawa, Y. Effects of the Difference Between the Refractive Indices of Constituent Materials on the Light Transmittance of Glass-Particle-Dispersed Epoxy-Matrix Optical Composites. *Philosophical Magazine B* **2002**, *82* (1), 1369–1386.

5. Iba, K.; Kagawa, Y. Light Transmittance of Continuous Fiber-Reinforced Composites: Analysis, Model Experiment and Parametric Study. *Philosophical Magazine B* **1998**, *78* (1), 37–52.

6. Weaver, K.; Stoffer, J.; Day, D. Preparation and Properties of Optically Transparent, Pressure-Cured PMMA Composites. *Polymer Composites* **1993**, *14* (6), 515–523.

7. Caseri, W. Nanocomposites of Polymers and Metals or Semiconductors: Historical Background and Optical Properties. *Macromolecular Rapid Communications* **2000**, *21* (11), 705–722.

8. Sandrock, M.; Wiggins, M.; Shirk, J. S.; Tai, H. W.; Ranade, A.; Baer, E.; Hiltner, A. A Widely Tunable Refractive Index in a Nanolayered Photonic Material. *Applied Physics Letters* **2004**, *84* (18), 3621–3623.

9. Yancey, S. E.; Zhong, W.; Heflin, J. R.; Ritter, A. L. The Influence of Void Space on Antireflection Coatings of Silica Nanoparticle Self-assembled Films. *Journal of Applied Physics* **2006**, *99*, 034313:1–10.

10. Arregui, F. J.; Dickerson, B.; Claus, R. O.; Matias, I. R.; Cooper, K. L. Polymeric Thin Films of Controlled Complex Refractive Index Formed by the Electrostatic Self-Assembled Monolayer Process. *Ieee Photonics Technology Letters* **2001**, *13* (12), 1319–1321.

11. Arregui, F. J.; Claus, R. O.; Cooper, K. L.; Fernandez-Valdivielso, C.; Matias, I. R. Optical Fiber Gas Sensor Based on Self-Assembled Gratings. *Journal of Lightwave Technology* **2001**, *19* (12), 1932–1937.

12. Shiue, J.; Matthewson, M. J.; Stupak, P. R. Rondinella, V. V. Effects of Silica Nanoparticle Addition to the Secondary Coating of Dual-Coated Optical Fibers. *Acta Materiallia* **2006**, *54*, 2631–2636.

13. Bohren, C. F.; Huffman, D. R. *Absorption and Scattering of Light by Small Particles*; Wiley-Interscience: New York, NY, 1983.

14. Lompado, A. Light Scattering by a Spherical Particle. http://diogenes.iwt.uni-bremen.de/vt /laser/wriedt/Mie_Type_Codes/body_mie_type_codes.html (accessed 2002).

15. Martin, J. E.; Wilcoxon, J. P.; Schaefer, D.; Odinek, J. Fast Aggregation of Colloidal Silica. *Physical Review A* **1990**, *41* (8), 4379–4391.

16. Torquato, S.; Truskett, T. M.; Debenedetti, P. G. Is Random Close Packing of Spheres Well Defined? *Physical Review Letters* **2000**, *84* (10), 2064–2067.

17. Lin, H.; Day, D. E.; Stoffer, J. O. Model for the Temperature Dependent Transmission of Optically Transparent Poly(methyl methacrylate) Composites. *Journal of Materials Research* **1993**, *8*, 364–370.

18. Kaplan, S. G.; Burnett, J. H. Optical Properties of Fluids for 248 and 193 nm Immersion Photolithography. *Applied Optics* **2006**, *45*, 1721–1724.

19. Weast, R.; Ed. *Handbook of Chemistry and Physics*; CRC Press: Cleveland, OH, 1974.

20. Malitson, L. H. Interspecimen Comparison of the Refractive Index of Fused Silica. *Journal of the Optical Society of America* **1965**, *55* (10), 1205–1209.

NO. OF
COPIES   ORGANIZATION

  1   DEFENSE TECHNICAL
 (PDF   INFORMATION CTR
 only)   DTIC OCA
          8725 JOHN J KINGMAN RD
          STE 0944
          FORT BELVOIR VA 22060-6218

  1   US ARMY RSRCH DEV &
          ENGRG CMD
          SYSTEMS OF SYSTEMS
          INTEGRATION
          AMSRD SS T
          6000 6TH ST STE 100
          FORT BELVOIR VA 22060-5608

  1   DIRECTOR
          US ARMY RESEARCH LAB
          IMNE ALC IMS
          2800 POWDER MILL RD
          ADELPHI MD 20783-1197

  1   DIRECTOR
          US ARMY RESEARCH LAB
          AMSRD ARL CI OK TL
          2800 POWDER MILL RD
          ADELPHI MD 20783-1197

  1   DIRECTOR
          US ARMY RESEARCH LAB
          AMSRD ARL CI OK T
          2800 POWDER MILL RD
          ADELPHI MD 20783-1197

          ABERDEEN PROVING GROUND

  1   DIR USARL
          AMSRD ARL CI OK TP (BLDG 4600)

22

NO. OF
COPIES ORGANIZATION

  2   VIRGINIA POLYTECHNIC INST
      & STATE UNIV
      PHYSICS DEPT
      R HEFLIN
      J RIDLEY
      ROBESON HALL (0435)
      BLACKSBURG VA 24061

ABERDEEN PROVING GROUND

  6   DIR USARL
      AMSRD ARL WM MA
        M VAN LANDINGHAM
        D O BRIEN
      AMSRD ARL WM MD
        J PATEL
        J SANDS
        P DEHMER
        A HSIEH

INTENTIONALLY LEFT BLANK.